

Scaling in Depth: Unlocking Robustness Certification on ImageNet

Kai Hu¹ Andy Zou¹ Zifan Wang¹ Klas Leino¹ Matt Fredrikson¹

Abstract

Notwithstanding the promise of Lipschitz-based approaches to *deterministically* train and certify robust deep networks, the state-of-the-art results only make successful use of feed-forward Convolutional Networks (ConvNets) on low-dimensional data, e.g. CIFAR-10. Because ConvNets often suffer from vanishing gradients when going deep, large-scale datasets with many classes, e.g., ImageNet, have remained out of practical reach. This paper investigates ways to scale up certifiably robust training to Residual Networks (ResNets). First, we introduce the *Linear ResNet* (LiResNet) architecture, which utilizes a new residual block designed to facilitate *tighter* Lipschitz bounds compared to a conventional residual block. Second, we introduce Efficient Margin MAXimization (EMMA), a loss function that stabilizes robust training by simultaneously penalizing worst-case adversarial examples from *all* classes. Combining LiResNet and EMMA, we achieve new *state-of-the-art* robust accuracy on CIFAR-10/100 and Tiny-ImageNet under ℓ_2 -norm-bounded perturbations. Moreover, for the first time, we are able to scale up deterministic robustness guarantees to ImageNet, bringing hope to the possibility of applying deterministic certification to real-world applications. We release our code on Github: <https://github.com/klasleino/gloro>.

1. Introduction

Deep neural networks have been shown to be vulnerable to well-crafted tiny perturbations to their inputs, also known as *adversarial examples* (Goodfellow et al., 2015; Szegedy et al., 2014). In the face of adversaries, it is common to consider a model’s *robustness*—that is, its ability to maintain consistent predictions within a norm-bounded ϵ -ball around an input, x . Prior works have proposed numerous

¹Carnegie Mellon University, Pittsburgh, USA. Correspondence to: Kai Hu <kaihu@andrew.cmu.edu>, Matt Fredrikson <mfredrik@cmu.edu>.

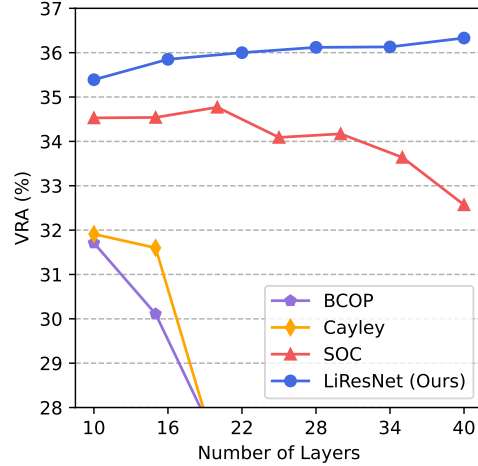


Figure 1. Plot of VRA—the number of points on which the model is both correct and certifiably robust—against the depth of the model. We compare our proposed architecture, LiResNet, with BCOP (Li et al., 2019a), SOC (Singla et al., 2022) and Cayley layers (Trockman & Kolter, 2021) on CIFAR-100, finding our architecture scales more favorably to deeper nets. See Appendix D for implementation details of this plot.

ways to improve robustness by regularizing the network during training, most notably by augmenting the data with dynamically generated adversarial examples (Goodfellow et al., 2015; Madry et al., 2018). However, this provides only an empirical defense, as models can still be vulnerable to stronger attacks that they have not seen before, e.g. an adaptive attack (Carlini & Wagner, 2017; Croce & Hein, 2020b). One solution to the problem above is to train a model that can *certify* its predictions within an ϵ -ball, which is therefore the focus of this paper.

Over the last few years, a wide body of literature addressing robustness certification has emerged (Cohen et al., 2019; Croce et al., 2019; Fromherz et al., 2021; Huang et al., 2021; Jordan et al., 2019; Lee et al., 2020; Leino et al., 2021; Li et al., 2019a;b; Singla et al., 2022; Tjeng et al., 2019; Trockman & Kolter, 2021; Wong & Kolter, 2018). To date, the methods that achieve by far the best certified performance are derived from *randomized smoothing* (Cohen et al., 2019); however, this provides only a *probabilistic* guarantee—which may generate a false positive claim around 0.1% of the time (Cohen et al., 2019)—and requires significant overhead for both evaluation and certification.

By contrast, *deterministic* certification may be preferred in safety-critical applications, e.g., malware detection and autonomous driving.

Because of the highly non-linear boundaries learned by a neural network, deterministically certifying the robustness of its predictions usually requires specialized training procedures that regularize the network for efficient certification, as post-hoc certification is either too expensive (Katz et al., 2017; Sinha et al., 2018) or too imprecise (Fromherz et al., 2021), particularly as the scale of the model being certified is increased. The most promising such approaches—in terms of both certified accuracy and efficiency—perform certification using Lipschitz bounds, meaning that the learning procedure must impose Lipschitz constraints on the layers during training, either through regularization (Leino et al., 2021) or orthogonalization (Trockman & Kolter, 2021).

While Lipschitz-based certification is efficient enough to perform robustness certification at scale (e.g., on ImageNet) in principle, the strict regularization it entails complicates training dynamics on large models required for such scales, and the layer-wise Lipschitz bounds it utilizes may become too loose in very deep models. As a result, state-of-the-art (deterministically) certified robustness is currently still achieved using relatively small feed-forward Convolutional Networks (ConvNets). Previous work has suggested that robust learning requires significant network capacity, both in general (Bubeck & Sellke, 2021), and for Lipschitz-based certification specifically (Leino, 2023). Despite this, ResNets (), which can usually go much deeper than ConvNets (and which achieve superior non-robust performance), have not been shown to outperform simple ConvNets with current certified approaches (Trockman & Kolter, 2021).

The goal of this work is to scale up certifiable robustness training from ConvNets to ResNets, with the aim of achieving higher *Verifiable Robust Accuracy* (VRA)—the percentage of points on which the model is both correct and certifiably robust. By realizing gains from more powerful architectures, we show it is possible to obtain non-trivial certified robustness on larger datasets like ImageNet, which, to our knowledge, has not yet been achieved by deterministic methods. Our results stem chiefly from two key innovations on *GloRo Nets* (Leino et al., 2021), a leading certified training approach.¹ First, we find that the residual branches used in the conventional ResNet architecture might not be a good fit for Lipschitz-based certification; instead, we find the key ingredient is to use a *linear* residual path (Figure 2) forming what we refer to as a *LiResNet* block. The motivation for this architecture development is covered in depth in Section 3.

Second, we find that the typical loss function used by GloRo

¹We choose GloRo Nets because they involve the least runtime and memory overhead compared to other leading certification methods, e.g., orthogonalization.

Nets in the literature may be suboptimal at pushing the decision boundary far away from the input in learning settings with large numbers of classes. Specifically, the standard GloRo loss penalizes possible adversarial examples from a *single* class at once (corresponding to the *closest* adversarial example), while we find a robust model can be more efficiently obtained by regularizing against adversarial examples from *all* possible classes at once, particularly when there are many classes. We thus propose *Efficient Margin MAXimization* (EMMA) loss for GloRo Nets, which simultaneously handles possible adversarial examples from any class. More details on the construction and motivation behind EMMA loss are provided in Section 4.

Using the LiResNet architecture and EMMA loss, we are able to (1) scale up deterministic robustness guarantees to ImageNet for the first time, and (2) substantially improve the VRAs on benchmark datasets used in prior work. In particular as exemplified in Figure 1, contradictory to the existing architectures that have been found no gains in VRA when going deeper, LiResNet demonstrates an effective use of the increasing capacity to learn more robust functions.

To summarize our contributions: (1) we introduce LiResNet, a ResNet architecture using a *linear residual branch* that better fits the Lipschitz-based certification approach; and (2) we propose EMMA loss to improve the training dynamics of robust learning with GloRo Nets. As a result, we achieve the new state-of-the-art VRAs on CIFAR-10 (65.1%), CIFAR-100 (36.3%), Tiny-ImageNet (27.4%) and ImageNet (14.2%) for ℓ_2 -norm-bounded perturbations. More importantly, to the best of our knowledge, for the first time we are able to scale up deterministic robustness guarantee to ImageNet, demonstrating the promise, facilitated by our architecture, of obtaining certifiably robust models in real-world applications.

2. Background

We are interested in certifying the predictions of a network $F(x) = \arg \max_j f_j(x)$ that classifies an input $x \in \mathbb{R}^d$ into m classes. We use the uppercase $F(x) : \mathbb{R}^d \rightarrow [m]$ to denote the integer class and the lowercase $f(x) : \mathbb{R}^d \rightarrow \mathbb{R}^m$ for the logits. A certifier checks for whether ϵ -local robustness (Definition 1) holds for an input x .

Definition 1 (ϵ -Local Robustness). A network $F(x)$ is ϵ -locally robust at an input x w.r.t norm, $\|\cdot\|$, if

$$\forall x' \in \mathbb{R}^d, \|x' - x\| \leq \epsilon \implies F(x') = F(x). \quad (1)$$

Existing certifiers are either *probabilistic* (i.e., guaranteeing robustness with bounded uncertainty) or *deterministic* (i.e., returning a certificate when a point is guaranteed to be robust). We focus on the latter in this paper and consider the ℓ_2 norm if not otherwise noted.

Lipschitz-based Certification. Certifying the robustness of a prediction can be achieved by checking if the margin between the logit of the predicted class and the others is large enough that no other class will surpass the predicted class on any neighboring point in the ϵ -ball. To this end, many prior works rely on calculating the Lipschitz Constant K (Definition 2) of the model to bound the requisite margin.

Definition 2 (K -Lipschitz Function). A function $h : \mathbb{R}^d \rightarrow \mathbb{R}^m$ is K -Lipschitz w.r.t $S \subseteq \mathbb{R}^d$ and norm, $\|\cdot\|$, if

$$\forall x, x' \in S. \|h(x) - h(x')\| \leq K\|x - x'\|. \quad (2)$$

Namely, K is the maximum change of a function’s output for changing the input in S . Notice that it is sufficient to use a *local* Lipschitz Constant K_{local} of the model, i.e. $S = \{x' \mid \|x' - x\| \leq \epsilon\}$ in Eq. 2, to certify robustness (Yang et al., 2020). However, the local bound is often computationally expensive and needs a bounded activation to be used in training (). Alternatively, one can compute a *global* Lipschitz Constant K_{global} , i.e. $S = \mathbb{R}^d$ in Eq. 2, and leverage the relation $K_{\text{global}} \geq K_{\text{local}}$ to certify any input at any radius ϵ . A global bound is more efficient at test time for certification because it only needs to be computed once and can be used for any input at any radius ϵ .² However, an arbitrary global bound can be vacuously large and thus not useful for positive certification.

GloRo. Among leading approaches that tighten the global Lipschitz constant during training for the purpose of certification (Leino et al., 2021; Singla et al., 2022; Trockman & Kolter, 2021), GloRo (Leino et al., 2021) is unique in that it naturally incorporates Lipschitz regularization into its loss rather than imposing direct constraints on the Lipschitz constant of each layer. As a result, it is more resource-efficient, and thus has the best potential to scale up to large-scale networks with high-dimensional inputs. GloRo computes the global Lipschitz constant, K_{ji} of the logit margin between the predicted class, j , and *every other class*, i , by taking the product of the Lipschitz constant of each constituent layer. Then, the so-called *GloRo Net* outputs $F(x) = j$ is $f_j(x) \geq \max_{i \neq j} \{f_i(x) + \epsilon K_{ji}\}$, or $F(x) = \perp$ otherwise. Thus, by design, whenever the GloRo Net does not output \perp , its prediction is guaranteed to be robust.

Robustness Needs More Capacity. Despite the fact that robust and correct predictions, i.e., VRA=100%, is achievable for many standard datasets (Yang et al., 2020), the state-of-the-art VRAs (which are achieved using Lipschitz-based certification) are far away from realizing this goal. Besides the fact Lipschitz-based certification is not exact

²Furthermore, when the network is *trained for certification with the global bound*, the global bound has the same certification potential as the local bound (Leino et al., 2021).

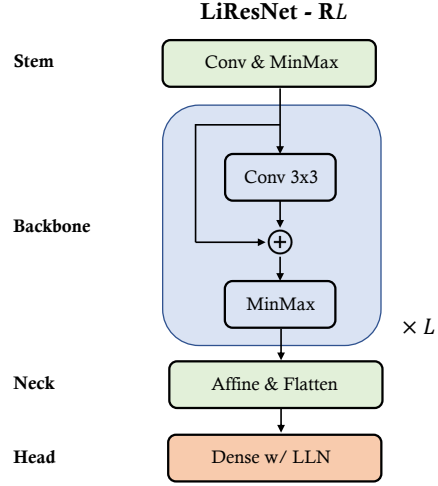


Figure 2. LiResNet Architecture.

and may falsely flag robust points, recent works have emphasized the role of network *capacity* in learning robust classifiers. Bubeck & Sellke (2021) showed that a smooth (and thus robust) decision boundary requires d times more parameters than learning a non-smooth one, where d is the ambient data dimension. In addition, to *tightly certify* a robust boundary with Lipschitz-based approaches, Leino (2023) demonstrated the need for extra capacity to learn smooth level curves around the decision boundary, which are shown to be necessary for tight certification.

Meanwhile, ResNets have been found to be more effective for scaling network depth compared to feed-forward ConvNets, and therefore efficiently leverage much larger network capacity to learn robust decision boundaries with smooth level curves. High-capacity ResNets have been shown to handily outperform basic ConvNets in terms of *clean accuracy* (i.e., ignoring robustness) on major research datasets () but similar success has never been observed for VRAs. For example, several papers find ResNets have lower VRAs on CIFAR-10 compared to ConvNets (Singla & Feizi, 2021; Trockman & Kolter, 2021). This empirical finding is seemingly at odds with the capacity arguments raised in the literature, however this may be due to unfavorable training dynamics of current approaches. This work aims to investigate the reasons behind this discrepancy to capture the potential of ResNet architectures, and scale up certified robustness to large datasets like ImageNet.

3. Constructing LiResNet

Motivation. The GloRo approach can easily be adapted from a ConvNet architecture to a ResNet architecture by simply adjusting how the Lipschitz constant is computed

where the residual and skip paths meet. Consider a conventional residual block $r(x)$ given by $r(x) = x + g(x)$, where the residual branch, g , is a small feed forward network, typically with 2-3 convolutional/linear layers paired with nonlinear activations. The Lipschitz constant, K_r , of $r(x)$, with respect to the Lipschitz constant, K_g , of $g(x)$ is upper-bounded by $K_r \leq 1 + K_g$.

Thus, a typical estimation of the residual block’s Lipschitz constant is $1 + K_g$. However, this is a loose estimation. To see this, let $u = \arg \max_x \|r(x)\|/\|x\|$, and observe that the bound is only tight if u and $r(u)$ point in the *same direction* in the representation space. This is presumably unlikely to happen, as random vectors are almost orthogonal in high-dimensional space. Thus, using $1 + K_g$ as the Lipschitz constant of $r(x)$ is unlikely to be tight even if K_g is tight.

The LiResNet Architecture. As discussed, the standard residual block is fundamentally challenging to obtain a tight Lipschitz bound on. Thus, we propose to use a *linear residual block*:

$$r_{\text{linear}}(x) = x + \text{Conv}(x)$$

Since $r_{\text{linear}}(x)$ is still a linear transformation of x , we can easily compute the equivalent convolution which has the same output as $r_{\text{linear}}(x)$. For example, consider the convolution with weights $\mathbf{W} \in \mathbb{R}^{(2k_0+1) \times (2k_0+1) \times n \times n}$ where $(2k_0 + 1)$ is the kernel size and n is the number of channels and zero padding k_0 . The weights of the equivalent convolution are then $\mathbf{W} + \delta$ where $\delta[k_0, k_0, i, i] = 1$ for all $i \in \{1, \dots, n\}$ and all other entries are set to zero. Thus, the Lipschitz constant of r_{linear} can be efficiently estimated using the power method (Farnia et al., 2019). Non-linearity of the network is then obtained by adding nonlinear activations (e.g., MinMax (Anil et al., 2019)) to the outputs of each residual block. By stacking multiple linear residual blocks (with interjecting activations), and including a stem, neck, and head, we obtain the *Linear ResNet* (LiResNet) architecture, illustrated in Figure 2.

4. Efficient Margin Maximization

Using LiResNet we are able to train deeper models on datasets with larger images and more classes. However, we observe that the original loss functions, i.e. Cross Entropy and TRADES, used by Leino et al. (2021) in training GloRo Nets become inefficient as the number of classes increases. One reason standard GloRo training may struggle with large numbers of classes is that the gradient signal it receives for combating adversarial examples is naturally sparse. Recall that the \perp logit of the GloRo net represents the maximum logit score achievable by any competing (i.e., not top-ranked) class within the adversary’s perturbation budget (see the illustration in Figure 4). As such, the value

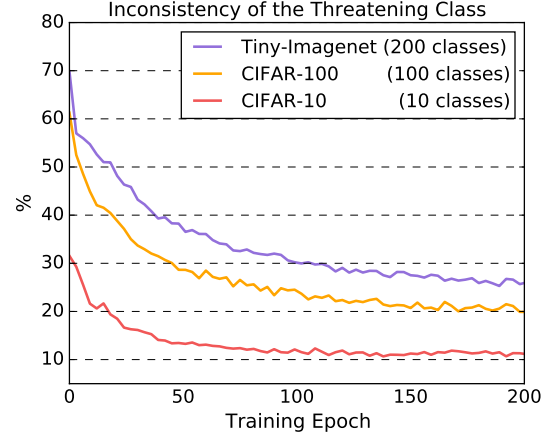


Figure 3. Plot of the percentage of instances at each epoch during training for which the *threatening* class (the one with the second-highest logit value) differs compared to the previous epoch (on the same instance). Numbers are reported on three datasets with 10, 100, and 200 classes using a GloRo LiResNet with TRADES loss.

of the \perp logit is determined by the logit corresponding to the *threatening* class—the one with the second highest value—adjusted by the appropriate margin. Especially when the Lipschitz constant is large, the \perp logit will be appreciably higher than the others. Thus, the loss will be largely attributed to the \perp logit, which will therefore send the strongest negative gradient signal.

Ultimately, this need not be a problem—by minimizing the loss originating from the *worst-case* adversary, the network successfully guards against *any* possible adversarial example. However, the \perp logit is only reduced by lowering the Lipschitz constant or reducing the threatening logit value, meaning that at each iteration, only one competing class faces a strong negative gradient signal, even if the threatening class is only slightly more competitive than the others. For example, in Figure 4, GloRo training at iteration t largely focuses on the decision boundary between class 1 and 3 even though class 2 is also competitive but slightly less so than class 3. Furthermore, the possibility arises, then, that the threatening class will alternate between competing classes in a sort of “whack-a-mole” during training.

Indeed, we find this phenomenon to be increasingly common as the number of classes grows. Figure 3 shows the fraction of instances at each epoch for which the threatening class differs from in the preceding epoch. In the initial 100 epochs, more than 30% instances from Tiny-ImageNet (containing 200 classes) have different threatening classes at each each iteration, while the same number for CIFAR-10 is only about 10%. At best, this contributes to making training with many classes less efficient, and at worst, it halts progress as work in one epoch is undone by the next.

To address this problem, we propose *Efficient Margin Max-*

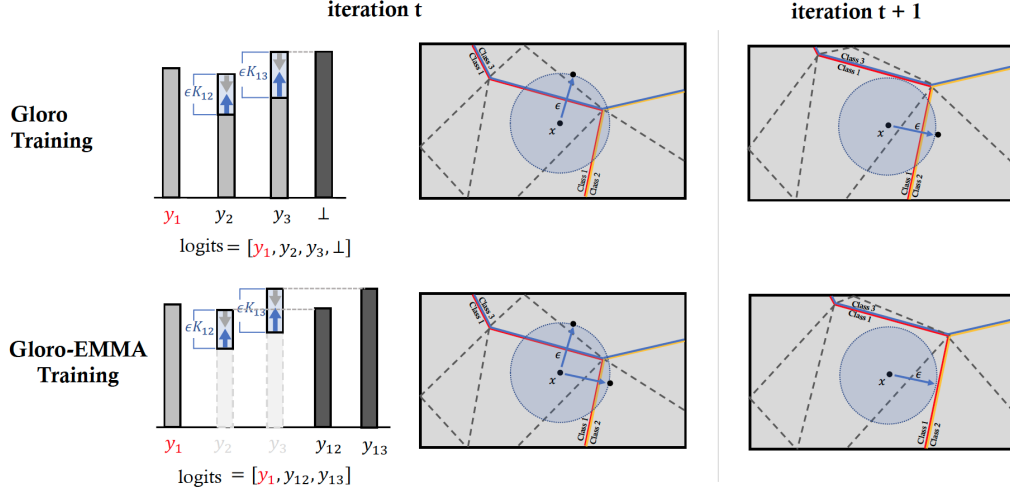


Figure 4. Comparison between the standard GloRo loss (CE or TRADES) and our proposed EMMA loss. GloRo loss constructs a \perp class to push the nearest decision boundary away while EMMA adds the perturbations to all rest classes (i.e. considering class 1 is the groundtruth) to efficiently push all boundaries away. At iteration $t + 1$, the network using EMMA loss is already robust while CE or TRADES may take more iterations to become robust.

imization (EMMA) loss (Definition 3) for training GloRo Nets. EMMA loss can be conceptualized as adding to each non-ground-truth class the maximum margin (ϵK_{yi}) the respective logit could gain on the ground truth logit within an ϵ neighborhood (illustrated in Figure 4). Effectively, this enables us to penalize adversarial examples from *all* classes simultaneously (as illustrated in Figure 4), leading to a less sparse gradient signal.

Definition 3 (Efficient Margin Maximization loss). Let $f(x)$ be the logit output, y be the ground truth label for x and K_{yi} be Lipschitz Constant of the margin between class y and i . We define EMMA loss as follows.

$$\text{EMMA}(f(x), y) = -\log \frac{\exp(f_y(x))}{\sum_{i \neq y} \exp(f_i(x) + \epsilon K_{yi})}.$$

In our evaluation in Section 5, we find that training with EMMA loss leads to higher VRA performance on robust classification tasks with many classes, e.g., CIFAR-100, Tiny-Imagenet, and Imagenet. Additionally, we find that EMMA loss appears to stabilize learning on deeper networks regardless of the number of classes.

5. Evaluation

In this section, we provide an empirical evaluation of LiResNet and EMMA loss in comparison to certifiably robust training approaches in prior works. We begin by comparing the best VRAs we achieve against the best VRAs reported in the literature in Section 5.1. Next, in Section 5.2, we run head-to-head comparisons between EMMA and typical GloRo losses as an ablation study to measure the empirical benefits of EMMA loss. Section 5.3 presents experiments

on networks of different depths, to shed light on the unique depth scalability of the LiResNet architecture. Finally in Section 5.4, we dive deeper into the ImageNet results, providing another novel observation regarding the impact of the number of classes on VRA.

The models in our evaluation either follow the architecture choices of prior work, or belong to a family of LiResNet architectures. To focus on the LiResNet, we do not experiment with variations in the stem, neck, or head. Thus, we refer to the particular architecture variations in our experiments by the number of number of LiResNet blocks, \mathbf{L} , and the number of input/output channels, \mathbf{W} . For example, **L6W128** refers to a LiResNet with 6 linear residual blocks with 128 channels each. See more details in Appendix A.

5.1. Improved VRA with LiResNet

We compare GloRo LiResNets trained with EMMA loss against the following baselines from the literature: standard GloRo Nets (i.e., with ConvNet architecture and CE/TRADES loss) (Leino et al., 2021), BCOP (Li et al., 2019b), Cayley (Trockman & Kolter, 2021), Local-Lip Net (Huang et al., 2021), and SOC with Householder and Certification Regularization (HH+CR) (Singla et al., 2022), selected for having been shown to surpass other approaches. We provide comparisons on CIFAR-10, CIFAR-100, and Tiny-ImageNet, using ℓ_2 perturbations with $\epsilon = 36/255$, following the standard setup in prior work. Additionally, we demonstrate the scalability of GloRo LiResNets by training on ImageNet with a certified radius of $\epsilon = 1$.

In addition to the VRA, we also report the clean accuracy (clean), and the empirical robust accuracy (PGD) using

Table 1. Comparing the proposed architecture LiResNet using the proposed loss EMMA against baseline methods. Verifiably Robust Accuracy (VRA) is the percentage of test points on which the model is both correct and certifiably robust so a higher VRA is better. Our Gloro Net results are better than the ones reported by [Leino et al. \(2021\)](#) and details to follow in Appendix A.

<i>method</i>	Architecture	Configuration	Clean (%)	PGD (%)	VRA (%)
CIFAR-10 ($\epsilon = 36/255$)					
BCOP	ConvNet	6C2F	75.1	67.3	58.3
Cayley	ConvNet	6C2F	75.3	67.7	59.2
Local-Lip Net	ConvNet	6C2F	77.4	70.4	60.7
SOC (HH+CR)	ConvNet	LipConv-15	76.4	-	63.0
Gloro Net	ConvNet	6C2F	77.0	69.2	60.0
Gloro Net (EMMA)	LiResNet	L6W128	76.5	70.6	63.7
Gloro Net (EMMA)	LiResNet	L18W256	78.1	72.0	65.1
CIFAR-100 ($\epsilon = 36/255$)					
BCOP	ConvNet	LipConv-10	45.4	-	31.7
Cayley	ConvNet	LipConv-10	45.8	-	31.9
SOC (HH+CR)	ConvNet	LipConv-20	47.8	-	34.8
Gloro Net (EMMA)	LiResNet	L6W128	49.6	43.4	35.4
Gloro Net (EMMA)	LiResNet	L18W256	51.2	44.7	36.3
Tiny-ImageNet ($\epsilon = 36/255$)					
Local-Lip Net	ConvNet	8C2F	36.9	33.3	23.4
Gloro Net	ConvNet	8C2F	35.5	32.3	22.4
Gloro Net (EMMA)	LiResNet	L6W128	37.8	33.8	27.0
Gloro Net (EMMA)	LiResNet	L18W256	40.7	36.3	29.2
ImageNet ($\epsilon = 1.0$)					
Gloro Net (EMMA)	LiResNet	L18W588	23.0	18.8	14.2

Auto-PGD ([Croce & Hein, 2020a](#)). For baselines, we directly report the results with best VRA (together with the PGD and clean accuracy) from the corresponding original papers. Table 1 details the comparison results and see Appendix A for further details on training.

On CIFAR-10, CIFAR-100 and Tiny-ImageNet, we find that LiResNet L6W128, which has about the same number of convolutional layers as compared to the ConvNets used by the baselines, is able to uniformly outperform other competitors. The larger LiResNet, i.e., L18W256, further improves the previous best VRAs to 65.1%, 36.3% and 29.2% on CIFAR-10, CIFAR-100 and Tiny-ImageNet, respectively.

There is no theoretical limitation of the baseline approaches that would prevent us from directly training them on ImageNet; however, practical resource constraints prevent us from training and wait until convergence. For example, baselines using orthogonalized kernels—e.g., Cayley, BCOP, and SOC—do not easily fit into memory with $224 \times 224 \times 3$ images, and local Lipschitz computation—e.g., Local-Lip Net—is both time and memory intensive. Thus, to the best of our knowledge, we are the first to report the VRA on ImageNet with a *deterministic* robustness guarantee.

5.2. Improved VRA with EMMA

This section demonstrates the empirical gains obtained by switching the typical loss used with GloRo, i.e. Cross Entropy (CE) and TRADES, to EMMA. For both ConvNets and LiResNets, we experiment on CIFAR-10, CIFAR-100 and Tiny-ImageNet and report VRAs in Table 2. ConvNets are modified to have same channel size (i.e. wider) as LiResNets and we end up achieving higher VRAs than ([Leino et al., 2021](#)). For all LiResNets, we adjust the configuration of the first convolution in the Tiny-ImageNet models to have the same output size compared to the CIFAR models, minimizing the impact of the image size on our conclusions (as the key variable in these experiments is the *number of classes*). Refer to Appendix B for remaining details and the clean accuracy of each model.

We see in Table 2 that the performance gain from switching CE or TRADES to EMMA becomes clear when the number of classes increases from 10 to 200. This observation aligns with our hypothesis used to motivate EMMA loss, discussed in Section 4, namely, that the rotating threatening class phenomenon observed during training (see Figure 3) may contribute to suboptimal learning.

Table 2. VRA performance (%) of a ConvNet and a LiResNet on three datasets with different loss functions.

loss	CE	TRADES	EMMA
CIFAR-10 ($\epsilon = 36/255$, 10 classes)			
ConvNet	63.0	62.8	62.6
LiResNet	63.8	63.5	63.7
CIFAR-100 ($\epsilon = 36/255$, 100 classes)			
ConvNet	32.8	32.8	33.9
LiResNet	32.7	33.0	35.4
Tiny-ImageNet ($\epsilon = 36/255$, 200 classes)			
ConvNet	23.3	23.3	26.0
LiResNet	23.3	23.5	27.0

Table 3. VRA (%) performance on CIFAR-10/100 with different architectures (L is the number of blocks in the model backbone). We use EMMA loss for GloRo training. A value of \times indicates that training was unable to converge.

Dataset	L	ConvNet	ResNet	LiResNet
CIFAR-10	6	62.6	60.0	63.7
	12	55.0	59.8	64.2
	18	\times	59.9	64.5
CIFAR-100	6	33.9	32.5	35.4
	12	28.2	32.5	35.9
	18	\times	32.8	36.0

5.3. Going Deeper with LiResNet

As depicted in Figure 1 from the introduction, the VRA obtained using GloRo LiResNets scales well as the depth of the model increases, while prior work has failed to further improve the best achievable VRA through additional layers. To further validate that the ability to successfully go deeper primarily comes from the structural improvement of linear residual branch in the LiResNet architecture—as opposed to being an advantage of the framework, GloRo, itself—we run head-to-head comparisons on CIFAR-10 and CIFAR-100 of GloRo Nets using (1) a feed-forward ConvNet architecture, (2) a conventional ResNet architecture, and (3) a LiResNet architecture. We train all three architectures with EMMA loss at three different depths. We report VRAs of these models in Table 3 (implementation details are given in Appendix C).

We see in Table 3 that very deep ConvNets may not be able to converge even on small-scale datasets like CIFAR-10 and CIFAR-100. Moreover, the VRA of both ConvNets and conventional ResNets do not benefit from the increasing network depth—in fact performance *decreases* as the network is made significantly deeper. By contrast, LiResNet is the only architecture under the same conditions that benefits from more layers, showing its unique promise for scalability. In Appendix C, we include more results with even deeper LiResNets on CIFAR-10, CIFAR-100 and Tiny-ImageNet.

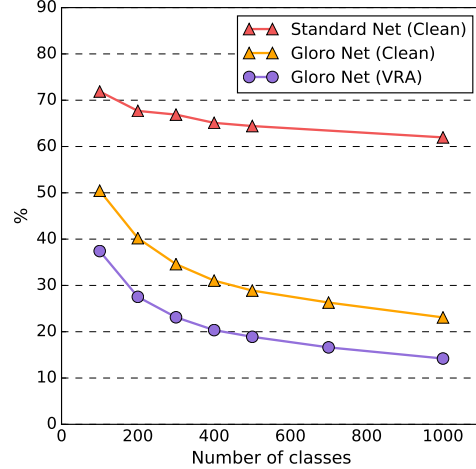


Figure 5. Plot of LiResNet performance on subsets of ImageNet with different number of classes.

5.4. Number of Classes vs. VRA

Despite the fact that EMMA loss improves the ability of GloRo Nets to handle learning problems with many classes, datasets with a large number of classes still stand out as particularly difficult for certified training. In principle, a data distribution with less classes is not guaranteed to have more separable features than more classes—indeed, the state-of-the-art clean accuracy for both CIFAR-10 and CIFAR-100 are comfortably in the high 90’s despite the large difference in the number of classes. However, training a certifiably robust model with many classes appears more difficult in practice (as observed, e.g., by the large performance gap between CIFAR-10 and CIFAR-100). To test this observation further, we provide an empirical study on various class-subsets of ImageNet to study the relationship between the number of classes and VRA.

We randomly shuffle the 1000 classes of ImageNet and select the first $100 \cdot k$ classes, where $k \in [10]$, to build a series of subsets for training and testing. For each value of k , we train a GloRo LiResNet with EMMA loss and report the clean accuracy and VRA (at $\epsilon = 1$) on the test set. For reference, we also train a standard (i.e., not robust) LiResNet with Cross Entropy and report its clean accuracy on the test set. The final results are shown in Figure 5 with additional details in Appendix E. Compared to the clean accuracy of a standard model, increasing the number of classes leads to a steeper drop in both the VRA and the clean accuracy of the robustly trained models. Specifically, while the performance of the standard model differs only by 10% between a 100-class subset and the full ImageNet, the performance of the GloRoNet (both clean accuracy and VRA), drops by 30%.

These results add weight to the observation that, even when

mitigated by EMMA loss, large numbers of classes present a particular challenge for certifiably robust learning. This may arise from the need to learn a 2ϵ -margin between all regions with different labels, which becomes progressively more challenging as boundaries between a growing number of classes become increasingly difficult to push off the data manifold.

6. Related Work

Tightening Lipschitz Bound. The closest line of work on improving VRAs with architecture redesign is the use of othornormalized convolution (Singla & Feizi, 2021; Trockman & Kolter, 2021), which is *exactly* 1-Lipschitz by construction. In a similar spirit, we introduce the linear residual branch in LiResNet to solve the overestimation of Lipschitz Constant in the conventional ResNet. Our linear residual layer compares favorably to othornormalized layers in a few key advantages. The linear branch is open to any affine transformation with no restriction on its kernel. Although there is no technical limitation that would prevent us from using othornormalized convolution in LiResNet, a standard convolution works favorably well in our experiments and is significantly less expensive than training with othornormalized ones. As is shown in Figure 1, it is worth mentioning that all prior works which attempt to scale up feed-forward ConvNets all fail to enjoy a gain of VRA, whereas the skip connection allows us to effectively utilize the increasing capacity and improve VRAs on various datasets.

Activation. Another design choice is to use Min-Max (Anil et al., 2019) activation to replace ReLU, as gradient-preserving activations have been proved to have tight Lipschitz bounds (Anil et al., 2019) and empirically improve VRAs on existing methods over ReLUs (Huang et al., 2021; Trockman & Kolter, 2021). Singla et al. (2022) introduces HouseHolder as a parameterized generalization of MinMax. Although we have not observed significant improvement of HouseHolder over MinMax in LiResNets, parameterizing activations to learn easy-to-certify level curves may be necessary to further improve any Lipschitz-based approach, as justified by Leino (2023).

Randomized Smoothing. Contradictory to the deterministic robustness guarantee focused in this paper, probabilistic guarantees, mostly based on *Raondmized Smoothing* (RS) (Cohen et al., 2019), have been long studied and experimented on ImageNet-scale models, motivating a set of smoothing-aware training approaches to further increase the robust radius (Carlini et al., 2022; Jeong et al., 2021; Salman et al., 2019; 2020). On ImageNet, RS indeed reports certifying more points than Gloro LiResNet at the same ϵ . However, the fundamental limitation of a probabilistic guarantee is the false positive results, meaning that adversarial

examples can go unchecked. Even a 0.1% false positive rate (FPR) is not affordable to many real-world security and financial applications. On the other hand, RS-based certification has order-of-magnitude larger computation overhead compared to Lipschitz-based certification. For the same example of FPR=0.1%, RS runs 100,000 extra inferences to certify 1 instance and the number grows up exponentially to achieve lower FPR (Cohen et al., 2019). This resource-consuming nature of RS-based certification in the end limits the type of applications one can deploy it for.

Fundamental Limitation in Robust Classification. Our motivation on EMMA and the empirical observations on the impact of class numbers to VRAs expose the hardness in scaling up robustness certification to real-world datasets. Training to be both robust and accurate has to balance the rewards between predicting the groundtruth and pushing away threatening boundaries, which often becomes precarious and tricky as the classes increase. In addition, the problem is potentially compounded by ambiguous or conflicting class labels, which may be indicative of a mismatch between the data distribution and the learning objective of *categorical accuracy*—and particularly its robust form. A number of mislabeled images have been identified in ImageNet (Beyer et al., 2020; Northcutt et al., 2021; Vasudevan et al., 2022; Yun et al., 2021), placing difficulties for robust classification. Moreover, real-word images are often not well-cropped input that only contains one semantically meaningful object. Robustly assigning only one label to an image with multiple objects, the often case in ImageNet, again limits the function networks can learn – the network either learn to not see the rest of objects or find that there is no way to be certifiably robust. In such cases, robust learning may be essentially limited unless alternate objectives (e.g., robust analogs of top- k accuracy (Leino & Fredrikson, 2021) and robust segmentation (Fischer et al., 2021)) are pursued.

7. Conclusion

In this work, we propose a new residual architecture, LiResNet, for training certifiably robust neural nets. LiResNet has a linear residual branch and thus has a tighter Lipschitz bound, allowing the model to scale much deeper. To stabilize robust training on deep networks, we introduce Efficient Margin MAXimization (EMMA), a loss function that simultaneously penalizes worst-case adversarial examples from all classes. Combining the two improvements, our models can achieve new state-of-the-art robust accuracy on CIFAR-10/100 and Tiny-ImageNet under ℓ -norm-bounded perturbations without sensitive choices of hyper-parameters. Furthermore, our model is the first to scale up deterministic robustness guarantees to ImageNet, showing a potential for large scale deterministic certification.

Acknowledgement

The work described in this paper has been supported by the Software Engineering Institute under its FFRDC Contract No. FA8702-15-D-0002 with the U.S. Department of Defense, as well as DARPA and the Air Force Research Laboratory under agreement number FA8750-15-2-0277.

References

- Anil, C., Lucas, J., and Gross, R. Sorting out Lipschitz function approximation. In *International Conference on Machine Learning (ICML)*, 2019.
- Beyer, L., Hénaff, O. J., Kolesnikov, A., Zhai, X., and Oord, A. v. d. Are we done with imagenet? *arXiv preprint arXiv:2006.07159*, 2020.
- Bubeck, S. and Sellke, M. A universal law of robustness via isoperimetry. In *NIPS*, 2021.
- Carlini, N. and Wagner, D. A. Towards evaluating the robustness of neural networks. In *IEEE Symposium on Security and Privacy (S&P)*, 2017.
- Carlini, N., Tramer, F., Kolter, J. Z., et al. (certified!!) adversarial robustness for free! *arXiv preprint arXiv:2206.10550*, 2022.
- Cohen, J., Rosenfeld, E., and Kolter, Z. Certified adversarial robustness via randomized smoothing. In *International Conference on Machine Learning (ICML)*, 2019.
- Croce, F. and Hein, M. Reliable evaluation of adversarial robustness with an ensemble of diverse parameter-free attacks. In *ICML*, 2020a.
- Croce, F. and Hein, M. Reliable evaluation of adversarial robustness with an ensemble of diverse parameter-free attacks. In *International Conference on Machine Learning (ICML)*, 2020b.
- Croce, F., Andriushchenko, M., and Hein, M. Provable robustness of ReLU networks via maximization of linear regions. In *International Conference on Artificial Intelligence and Statistics (AISTATS)*, 2019.
- Dosovitskiy, A., Beyer, L., Kolesnikov, A., Weissenborn, D., Zhai, X., Unterthiner, T., Dehghani, M., Minderer, M., Heigold, G., Gelly, S., et al. An image is worth 16x16 words: Transformers for image recognition at scale. *ICLR 2021*, 2020.
- Farnia, F., Zhang, J., and Tse, D. Generalizable adversarial training via spectral normalization. In *International Conference on Learning Representations (ICLR)*, 2019.
- Fischer, M., Baader, M., and Vechev, M. Scalable certified segmentation via randomized smoothing. In Meila, M. and Zhang, T. (eds.), *Proceedings of the 38th International Conference on Machine Learning*, volume 139 of *Proceedings of Machine Learning Research*, pp. 3340–3351. PMLR, 18–24 Jul 2021.
- Fromherz, A., Leino, K., Fredrikson, M., Parno, B., and Păsăreanu, C. Fast geometric projections for local robustness certification. In *International Conference on Learning Representations (ICLR)*, 2021.
- Goodfellow, I. J., Shlens, J., and Szegedy, C. Explaining and harnessing adversarial examples, 2015.
- Goyal, P., Dollár, P., Girshick, R., Noordhuis, P., Wesolowski, L., Kyrola, A., Tulloch, A., Jia, Y., and He, K. Accurate, large minibatch sgd: Training imagenet in 1 hour. *arXiv preprint arXiv:1706.02677*, 2017.
- Huang, Y., Zhang, H., Shi, Y., Kolter, J. Z., and Anandkumar, A. Training certifiably robust neural networks with efficient local lipschitz bounds. In *NIPS*, 2021.
- Jeong, J., Park, S., Kim, M., Lee, H.-C., Kim, D.-G., and Shin, J. Smoothmix: Training confidence-calibrated smoothed classifiers for certified robustness. *Advances in Neural Information Processing Systems*, 34:30153–30168, 2021.
- Jordan, M., Lewis, J., and Dimakis, A. G. Provable certificates for adversarial examples: Fitting a ball in the union of polytopes. In *Neural Information Processing Systems (NIPS)*, 2019.
- Katz, G., Barrett, C. W., Dill, D. L., Julian, K., and Kochenderfer, M. J. Reluplex: An efficient SMT solver for verifying deep neural networks. In *International Conference on Computer-Aided Verification (CAV)*, 2017.
- Kingma, D. P. and Ba, J. Adam: A method for stochastic optimization. *arXiv preprint arXiv:1412.6980*, 2014.
- Langley, P. Crafting papers on machine learning. In Langley, P. (ed.), *Proceedings of the 17th International Conference on Machine Learning (ICML 2000)*, pp. 1207–1216, Stanford, CA, 2000. Morgan Kaufmann.
- Lee, S., Lee, J., and Park, S. Lipschitz-certifiable training with a tight outer bound. In *Neural Information Processing Systems (NIPS)*, 2020.
- Leino, K. Limitations of piecewise linearity for efficient robustness certification. 2023.
- Leino, K. and Fredrikson, M. Relaxing local robustness. In *Neural Information Processing Systems (NIPS)*, 2021.

- Leino, K., Wang, Z., and Fredrikson, M. Globally-robust neural networks. In *International Conference on Machine Learning (ICML)*, 2021.
- Li, Q., Haque, S., Anil, C., Lucas, J., Grosse, R., and Jacobsen, J.-H. Preventing gradient attenuation in lipschitz constrained convolutional networks. *Conference on Neural Information Processing Systems*, 2019a.
- Li, Q., Haque, S., Anil, C., Lucas, J., Grosse, R. B., and Jacobsen, J.-H. Preventing gradient attenuation in lipschitz constrained convolutional networks. In *Neural Information Processing Systems (NIPS)*, 2019b.
- Loshchilov, I. and Hutter, F. Sgdr: Stochastic gradient descent with warm restarts. *arXiv preprint arXiv:1608.03983*, 2016.
- Madry, A., Makelov, A., Schmidt, L., Tsipras, D., and Vladu, A. Towards deep learning models resistant to adversarial attacks. In *International Conference on Learning Representations (ICLR)*, 2018.
- Northcutt, C. G., Athalye, A., and Mueller, J. Pervasive label errors in test sets destabilize machine learning benchmarks. *arXiv preprint arXiv:2103.14749*, 2021.
- Paszke, A., Gross, S., Massa, F., Lerer, A., Bradbury, J., Chanan, G., Killeen, T., Lin, Z., Gimelshein, N., Antiga, L., et al. Pytorch: An imperative style, high-performance deep learning library. *Advances in neural information processing systems*, 32, 2019.
- Salman, H., Li, J., Razenshteyn, I., Zhang, P., Zhang, H., Bubeck, S., and Yang, G. Provably robust deep learning via adversarially trained smoothed classifiers. *Advances in Neural Information Processing Systems*, 32, 2019.
- Salman, H., Sun, M., Yang, G., Kapoor, A., and Kolter, J. Z. Denoised smoothing: A provable defense for pretrained classifiers. *Advances in Neural Information Processing Systems*, 33:21945–21957, 2020.
- Shao, J., Hu, K., Wang, C., Xue, X., and Raj, B. Is normalization indispensable for training deep neural network? *Advances in Neural Information Processing Systems*, 33: 13434–13444, 2020.
- Singla, S. and Feizi, S. Skew orthogonal convolutions. In Meila, M. and Zhang, T. (eds.), *Proceedings of the 38th International Conference on Machine Learning*, volume 139 of *Proceedings of Machine Learning Research*, pp. 9756–9766. PMLR, 18–24 Jul 2021.
- Singla, S., Singla, S., and Feizi, S. Improved deterministic l2 robustness on cifar-10 and cifar-100. In *ICLR*, 2022.
- Sinha, A., Namkoong, H., and Duchi, J. Certifiable distributional robustness with principled adversarial training. In *International Conference on Learning Representations (ICLR)*, 2018.
- Szegedy, C., Zaremba, W., Sutskever, I., Bruna, J., Erhan, D., Goodfellow, I. J., and Fergus, R. Intriguing properties of neural networks. In *International Conference on Learning Representations (ICLR)*, 2014.
- Tjeng, V., Xiao, K. Y., and Tedrake, R. Evaluating robustness of neural networks with mixed integer programming. In *International Conference on Learning Representations (ICLR)*, 2019.
- Trockman, A. and Kolter, J. Z. Orthogonalizing convolutional layers with the cayley transform. In *International Conference on Learning Representations (ICLR)*, 2021.
- Vasudevan, V., Caine, B., Gontijo-Lopes, R., Fridovich-Keil, S., and Roelofs, R. When does dough become a bagel? analyzing the remaining mistakes on imagenet. *arXiv preprint arXiv:2205.04596*, 2022.
- Wong, E. and Kolter, Z. Provable defenses against adversarial examples via the convex outer adversarial polytope. In *ICML*, 2018.
- Yang, Y.-Y., Rashtchian, C., Zhang, H., Salakhutdinov, R. R., and Chaudhuri, K. A closer look at accuracy vs. robustness. In *Neural Information Processing Systems (NIPS)*, 2020.
- Yun, S., Oh, S. J., Heo, B., Han, D., Choe, J., and Chun, S. Re-labeling imagenet: From single to multi-labels, from global to localized labels. In *Proceedings of the IEEE/CVF Conference on Computer Vision and Pattern Recognition (CVPR)*, pp. 2340–2350, June 2021.
- Zhang, H., Dauphin, Y. N., and Ma, T. Fixup initialization: Residual learning without normalization. *ICLR*, 2019.

Appendix

A. Implementation Details for Table 1

A.1. Training details

Dataset details The input resolution is 32 for CIFAR10/100, 64 for Tiny-ImageNet and 224 for ImageNet respectively. We apply a simple data augmentation to all datasets: random cropping and random horizontal flipping.

Platform details Our experiments were conducted on an 8-GPU (Nvidia A100) machine with 64 CPUs (Intel Xeon Gold 6248R). Each experiment on CIFAR10/100 and Tiny-ImageNet takes one GPU and each experiment on ImageNet takes 8 GPUs. Our implementation is based on PyTorch (Paszke et al., 2019).

Training details On the first 3 datasets, all models are trained with the Adam optimizer (Kingma & Ba, 2014) with a batch size of 256 and a learning rate of 10^{-3} for 800 epochs. We use a cosine learning rate decay (Loshchilov & Hutter, 2016) with linear warmup (Goyal et al., 2017) in the first 20 epochs. On ImageNet, we only change the batch size to 1024 and training epochs to 400.

We use $\epsilon = 36/255$ for CIFAR10/100 and Tiny-ImageNet and $\epsilon = 1$ following a linear rule:

$$\epsilon_{\text{ImageNet}} = \frac{\epsilon_{\text{CIFAR}}}{R_{\text{CIFAR}}} \times R_{\text{ImageNet}} = \frac{36/255}{32} \times 224 \approx 1.$$

for certification during validation. During training, we schedule the training ϵ to ramp up from small values and slightly overshoot the test epsilon. Let the total number of epochs be T and the test certification radius be ϵ , we use

$$\epsilon_{\text{train}}(t) = \left(\min\left(\frac{2t}{T}, 1\right) \times 1.4 + 0.1 \right) \epsilon$$

at epoch t . As a result, $\epsilon_{\text{train}}(t)$ begins at 0.1ϵ and increases linearly to 1.5ϵ before arriving halfway through the training. Later, ϵ_{train} remains 1.5ϵ to the end.

A.2. Model architecture details

Model stem is used to convert the input images into feature maps. On CIFAR10/100, we use a convolution with kernel size 5, stride 2, and padding 2, followed by a MinMax activation as the stem. On Tiny ImageNet, we use a convolution with kernel size 7, stride 4, and padding 3, followed by a MinMax activation as the stem. On ImageNet, we follow the ViT-like patching (Dosovitskiy et al., 2020) and use a convolution with kernel size 14, stride 14, and padding 0, followed by a MinMax activation as the stem. Thus the output feature map size from the stem layer is 16×16 for all 4 datasets. The number of filters used in the convolution is equal to the model width W .

Model backbone is used to transform the feature maps. It is a stack of L LiResNet blocks followed by the MinMax activation, i.e., $(\text{LiResNet block} \rightarrow \text{MinMax}) \times L$. We keep the feature map resolutions and the number of channels constant in the model backbone. We find some tricks in normalization-free residual network studies (Shao et al., 2020; Zhang et al., 2019) can improve the performance of our LiResNet as our method is also a normalization-free residual network. Specifically, we add an affine layer β that applies channel-wise learnable multipliers to each channel of the feature map (similar to the affine layer of batch normalization) and a scaler of $1/\sqrt{L}$ to the residual branch where L is the number of blocks:

$$y = x + \frac{1}{\sqrt{L}} \beta \text{Conv}(x)$$

Model neck is used to convert the feature maps into a feature vector. In our implementation, the model neck is a 2 layer network. The first layer is a convolution layer with kernel size 4, stride 4, and padding 0, followed by a MinMax activation.

Table 4. Clean accuracy and VRA performance (%) of a ConvNet and a LiResNet on three datasets with different loss functions

<i>loss</i>	Cross Entropy		TRADES		EMMA	
	Clean (%)	VRA (%)	Clean (%)	VRA (%)	Clean (%)	VRA (%)
CIFAR-10 ($\epsilon = 36/255$, 10 classes)						
ConvNet	77.9	63.0	77.9	62.8	74.7	62.6
LiResNet	80.0	63.8	79.6	63.5	76.5	63.7
CIFAR-100 ($\epsilon = 36/255$, 100 classes)						
ConvNet	54.0	32.8	54.0	32.8	46.1	33.9
LiResNet	54.9	32.7	55.0	33.0	49.6	35.4
Tiny-ImageNet ($\epsilon = 36/255$, 200 classes)						
ConvNet	40.4	23.3	40.4	23.3	36.3	26.0
LiResNet	41.5	23.3	41.8	23.5	39.1	27.0

The number of input channels is the model width W and the number of output channels is $2W$. Then we reshape the feature map tensor into a vector. The second layer is a dense layer with output dimension d where $d = 512$ for the three small datasets (CIFAR10/100 and Tiny-ImageNet) and $d = 2048$ for ImageNet.

Model head is used to make classification predictions. We apply the last layer normalization (LLN) proposed by Singla et al. (2022) to the head.

A.3. Metric details

We report the clean accuracy, i.e., the accuracy without verification on non-adversarial inputs, the PGD accuracy, i.e., the accuracy under adversarial perturbations found via the PGD attack (Madry et al., 2018), and the verified-robust accuracy (VRA), i.e., the fraction of points that are both correctly classified and certified as robust. Our results are averaged over 5 runs for CIFAR10/100 and TinyImageNet and 3 runs for ImageNet.

B. Details for Table 2

In Table 2, we use an L6W128 configuration, i.e., the backbone has 6 blocks and the number of filters is 128. For ConvNet, the only difference is that the LiResNet block is replaced by a convolution of kernel 3, stride 1, and padding 1. All other settings are the same. Table 4 is a more detailed version of Table 2 with the clean accuracy.

C. Details for Table 3

In Table 3, we use the configuration of W128, i.e., the number of channels in the backbone is 128. The only difference between conventional ResNet and LiResNet is the block. The block for conventional ResNet is

$$y = x + \beta \text{Conv}(\text{MinMax}(\text{Conv}(x)))$$

where β is the affine layer. We find use zeros to initialize β works the best for conventional ResNet. The number of input and output channels of the two convolution layers are the same as that of the LiResNet block. Table 5 is a more detailed version of Table 3 with clean accuracy.

D. Details for Figure 1

We make LiResNet further deeper and study how network depth influences the performance on CIFAR-10/100 and Tiny-ImageNet. Table 6 shows the clean accuracy and VRA of LiResNet (with EMMA loss) on three datasets. All models use a W128 configuration, i.e., the number of convolutional channels is 128. On CIFAR-10/100, the VRA performance of the LiResNet generally improves with depth. On Tiny-ImageNet, the performance remains with the increase of depth.

Figure 1 compares the VRA performance of LiResNet with some existing method for verification robustness on CIFAR-100

Table 5. Clean accuracy and VRA (%) performance on CIFAR-10/100 with different architectures (L is the number of blocks in the model backbone). We use EMMA loss for Gloro training. NC stands for not converging at the end.

Dataset	L	ConvNet		ResNet		LiResNet	
		Clean(%)	VRA(%)	Clean(%)	VRA(%)	Clean(%)	VRA(%)
CIFAR-10	6	74.7	62.6	72.6	60.0	76.5	63.7
	12	65.5	55.0	72.5	59.8	77.0	64.2
	18	NC	NC	72.4	59.9	77.2	64.5
CIFAR-100	6	46.1	33.9	45.5	32.5	49.4	35.4
	12	37.8	28.2	45.1	32.5	50.1	35.9
	18	NC	NC	45.5	32.8	50.3	36.0

Table 6. Clean accuracy and VRA (%) performance of LiResNet of different depths (L is the number of blocks in the model backbone).

L	CIFAR10		CIFAR100		Tiny-ImageNet	
	Clean(%)	VRA(%)	Clean(%)	VRA(%)	Clean(%)	VRA(%)
6	76.5	63.7	49.4	35.4	39.1	27.1
12	77.0	64.2	50.1	35.9	39.5	27.3
18	77.2	64.5	50.3	36.0	39.6	27.3
24	77.2	64.5	50.5	36.1	39.4	27.3
30	77.5	64.6	50.4	36.1	39.4	27.3
36	77.7	64.9	55.6	36.3	39.3	27.2

(i.e., the 5th of Table 6). The numbers of these methods are taken from their best-reported configurations. The VRA performance of these methods degrades at certain depths, limiting the maximum model capacity of the methods.

E. Details for Figure 5

Table 7 shows the clean accuracy as well as the VRA to plot Figure 5 against a different number of classes. All models in this table uses an L18W588 configuration. To see how the partitioning of subsets influences the results. We use two seeds (i.e., 2023 and 2022 as shown in the table) to shuffle the classes and repeat the experiments. “-” means not running the experiments as the performance difference between different seeds is small enough.

We would like to provide some observations from this experiment. The VRA performance of the ImageNet 100-class and 200-class subsets is close to the VRA of CIFAR-100 and Tiny-ImageNet respectively as shown in Figure 6, even though we use different subsets. This might imply that the number of classes is a major factor to determine the VRA of our method across datasets.

Secondly, the logarithm of the accuracy is roughly linear to the logarithm of the number of classes. Figure 7 is a log log plot of Figure 7, and all three curves are roughly linear, which implies that the relationship between the accuracy A and the number of classes N is $A \propto N^{-k}$ for some positive constant k . The constant k for certifiable training is much larger than that constant for standard training. We are not clear if these observations can generalize to other datasets and architectures, which is a future work. However, they provide a strong hint that the number of classes is an important issue for this task.

F. Going Wider with LiResNet

We study how network width (i.e., the number of) can influence the performance of LiResNet on CIFAR-10 and CIFAR-100. Table 8 shows the results. All models use a L18 configuration. Unlike the network depth, increasing the width can stably improve the model performance within a certain range.

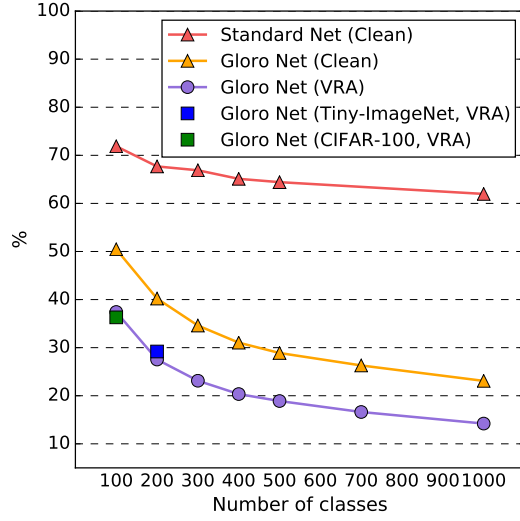


Figure 6. Curves of the LiResNet performance on subsets of ImageNet with a different number of classes. From top to bottom is the accuracy of standard classification training, the clean accuracy of certifiable training, and the VRA ($\epsilon = 1$) of certifiable training respectively. We additionally include the best VRAs ($\epsilon = 36/255$) on CIFAR-100 and Tiny-ImageNet in the graph.

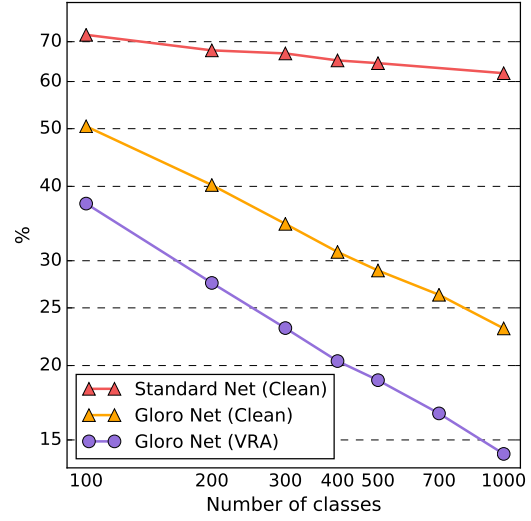


Figure 7. A log-log curve of Figure 1 to show the LiResNet performance on subsets of ImageNet with different number of classes. Both the x and y axis are in logarithm scale.

Table 7. Clean accuracy and VRA (%) performance of LiResNet L18W588 on subsets of ImageNet with different number of classes.

classes	seed=2023		seed=2022	
	Clean(%)	VRA(%)	Clean(%)	VRA(%)
100	50.5	37.4	46.9	34.3
200	40.2	27.5	37.7	26.5
300	34.6	23.1	33.8	22.7
400	31.0	20.4	30.7	20.3
500	28.9	18.9	28.7	18.8
700	26.3	16.6	-	-
1000	23.0	14.2	-	-

Table 8. VRA (%) of LiResNet of different widths (W).

W	CIFAR-10	CIFAR-100
64	63.4	35.2
128	64.5	36.0
256	65.1	36.3